Università degli Studi Mediterranea di Reggio Calabria
Archivio Istituzionale dei prodotti della ricerca

A Simple Procedure to Design Virtual Experiments for Microwave Inverse Scattering

(Article begins on next page)

07 February 2025

A Simple Procedure to Design Virtual Experiments for Microwave Inverse Scattering

Martina T. Bevacqua, Roberta Palmeri, Tommaso Isernia and Lorenzo Crocco

Abstract—In a virtual experiment, the data available to solve an inverse scattering problem are linearly combined in order to make the inversion task simpler. This goal is achieved by conditioning contrast sources radiating the scattered fields and exploiting their properties in the inversion procedure, for instance by devising data-driven approximations or regularization schemes. In this framework, the design of a virtual experiment amounts to determine the coefficients ruling the recombination of the available data. In this paper, we present a general and simple procedure to design virtual experiments capable of enforcing contrast sources with desired properties. The proposed procedure is computationally straightforward and stable, as it does not require an explicit inversion and regularization process, and just consists in the evaluation of the adjoint solution of an auxiliary problem. The design approach is tested in the case of VE enforcing circularly symmetric contrast sources and the corresponding inversion procedure is assessed using both simulated and experimental data.

Index Terms— adjoint solution, microwave imaging, inverse scattering problem, virtual scattering experiments, orthogonality sampling method, algebraic reconstruction method.

I. INTRODUCTION

IN microwave imaging, the *virtual* experiments (VE) are defined as a new set of experiments whose realization does not require physical measurements, but is obtained through a suitable (numerical) rearrangement of the measurements already performed to probe an unknown target [1]-[3]. In so doing, the VE do not aim at introducing new information, but rather at implicitly enforcing peculiar properties of the (unknown) contrast sources (and/or the total fields) induced in the imaging domain by the interaction between the target and the probing (incident) fields.

By taking these imposed properties into account, it is possible to conveniently recast the inverse scattering problem and counteract the pitfalls arising in its solution, namely, the ill-posedness and the non-linearity [4]. For instance, thanks to this approach, a new data-driven linear approximation having an extended validity range as compared to the traditional Born approximation [1] has been developed and effective non-linear inversion methods based on algebraic inversion formulas [2] or

peculiar forms of regularization [3] have been proposed.

In practice, to turn a set of scattering experiments into a VE, one has to determine the coefficients ruling a superposition of the measured scattered fields that matches the *virtual* scattered field one wants to enforce and which is in turn radiated by the desired *virtual* contrast source. To cope with this design (or synthesis) problem, some overlooked pieces of information arising from the linear sampling method (LSM) and the factorization method (FM) [6] have been so far exploited [1]-[3]. More recently, orbital angular momentum has also been exploited in linearized microwave imaging [7] and in particular in the VE framework [8].

While successful to demonstrate the effectiveness of the VE framework, the VE design procedures used so far requires the solution of a linear ill-posed inverse problem, thus being subject to possible inaccuracies. In fact, instabilities in the inversion process may be such to lose the direct control on the contrast sources, whose behaviour is the actual ultimate goal of the VE design.

In this paper, we introduce a new and general VE design procedure that (partially) overcomes the above issues and determines the superposition coefficients in a simpler and more effective way. Such a new approach is general as it allows to possibly design VE contrast sources other than focused ones. The proposed approach is also straightforward as, by virtue of the adjoint operator method introduced in the '60s by Dymskii [9],[10], it provides a convenient approximate solution to the synthesis problem, without requiring an explicit inversion and regularization process. Moreover, and most important for our purpose, we show that the proposed procedure is capable to better design and control the *virtual* contrast source induced within the unknown target by the synthesized VE. Finally, once particularized to the case of circularly symmetric VE currents, the new approach is also related to a well-known qualitative imaging technique, the orthogonality sampling method (OSM) [11]-[13], so that it can be used to provide an estimate of the support (i.e., location and shape) of the targets, which represents a convenient piece of information to further simplify the solution of the inverse scattering problem.

The paper is organized as follows. In Section II, the inverse scattering problem is formulated and the basic VE definitions

are briefly recalled. In Section III, the new VE design procedure is outlined. In Section IV, the new procedure is detailed for the case of VE whose contrast sources are designed to exhibit a circular symmetry. In Section V, we assess the capabilities of the new design procedure showing that it outperforms previous strategies. Finally, Section VI discusses and shows the added value of the proposed procedure when dealing with actual inversion. In particular, the effectiveness of the proposed strategy is verified against synthetic and experimental data by exploiting the designed "circularly symmetric" VE to set the direct algebraic reconstruction method [2]. Conclusions follow. Throughout the paper we consider the canonical 2D scalar problem (TM polarized fields), linear media, and we assume and drop the time harmonic factor $exp\{j\omega t\}$.

II. INVERSE SCATTERING PROBLEM AND VIRTUAL SCATTERING EXPERIMENTS FRAMEWORK

A. Statement of the inverse scattering problem

Let Ω denote the region under test where the targets are located. The contrast function $\chi(\boldsymbol{r}) = \frac{\epsilon_s(\boldsymbol{r})}{\epsilon_b(\boldsymbol{r})} - 1$, $\boldsymbol{r} = (x, y) \in \Omega$ relates the unknown complex permittivity of the scatterers $\epsilon_s(\boldsymbol{r})$, to that of the host medium ϵ_b. Without loss of generality, let us assume that the host medium is homogeneous.

The scatterers are probed by the incident fields $E_i(\boldsymbol{r}, \boldsymbol{r_t})$ radiated by N antennas located in $\boldsymbol{r_t} \in \Gamma$, with $t = 1, .., N$ and Γ being a curve which is external to Ω. The resulting scattered fields $E_s(\boldsymbol{r_m}, \boldsymbol{r_t})$ are measured by M antennas positioned at $\boldsymbol{r_m} \in \Gamma$, with $m = 1, .., M$ (see Figure 1).

Under the above assumptions, the equations describing the scattering problem can be expressed in integral form as [4],[14]:

$$E_s(\boldsymbol{r_m}, \boldsymbol{r_t}) = \int_\Omega G_b(\boldsymbol{r_m}, \boldsymbol{r'}) W(\boldsymbol{r'}, \boldsymbol{r_t}) d\boldsymbol{r'} = \mathbb{A}_e[W]$$

(1.a)

$$W(\boldsymbol{r}, \boldsymbol{r_t}) = \chi(\boldsymbol{r}) E_i(\boldsymbol{r}, \boldsymbol{r_t}) + \chi(\boldsymbol{r}) \int_\Omega G_b(\boldsymbol{r}, \boldsymbol{r'}) W(\boldsymbol{r'}, \boldsymbol{r_t}) d\boldsymbol{r'}$$
$$= \chi E_i + \chi \mathbb{A}_i[W]$$

(1.b)

where W is the contrast source induced in the target, and G_b is the Green's function pertaining to the background medium. $\mathbb{A}_e : L^2(\Omega) \to L^2(\Gamma)$ and $\mathbb{A}_i : L^2(\Omega) \to L^2(\Omega)$ are the short notations for the corresponding integral radiation operators.

The problem cast by Eqs. (1) is non-linear, as W depends on the unknown of the problem, i.e., the contrast χ. Moreover, it is also ill-posed, due to the properties of the radiation operator $\mathbb{A}_e$ [15]. Indeed, as discussed in [16], for both cases of single and multiple illuminating incident waves, the scattering operator is compact. As the inverse of a compact operator cannot be continuous, the inverse scattering problem is ill-posed. Then, small variations of the scattered field data produce unbounded variations of the corresponding solutions. Another important consequence is that the scattered fields admit a finite-
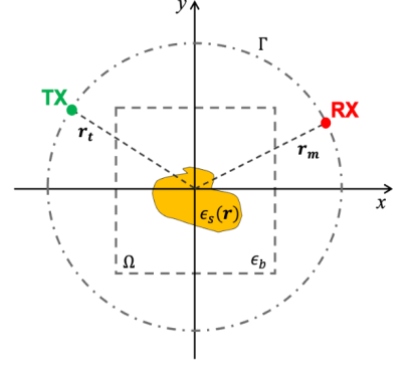

Figure 1. Pictorial view of the domain of interest and the transmitters and receivers locations.

dimensional representation within any required accuracy [16]. By virtue of the above, in any scattering experiment one deals with a finite amount of independent data (no matter how many samples one is collecting). Also, by considering the operator relating the primary source to the field inside domain under test, it also follows that only a finite number of independent scattering experiments can be performed. As a consequence, care has to be taken in choosing the number and positions of transmitting and receiving probes, as their placement (and number) affects the possibility of collecting all the available information, in a non-redundant fashion. In the paper, the conceptual framework developed in [16] is adopted.

B. The Virtual Experiments Framework

From Eq. (1.b), it can be noted that, for a fixed contrast function, the relationship between the contrast source and the incident field is linear. As Eq. (1.a) is linear too, it follows that, for any given scatterer, the relationship between scattered field and the incident field is linear as well.

The concept of VE is based on this simple observation, which entails that the information arising from multiple scattering experiments can be re-organized in a different possibly more convenient way by means of a linear superposition of the incident fields [1]-[3].

By repeatedly applying this simple procedure (that is by considering several sets of superposition coefficients) it is possible to generate a set of virtual scattering experiments, with no need of additional measurements.

From a mathematical point of view, a VE is identified by a *virtual* incident field $\mathcal{E}_i$ obtained through a linear superposition of the known incident fields according to the *virtual excitation coefficients* $\boldsymbol{\alpha} = (\alpha_1, \dots, \alpha_N)$:

$$\mathcal{E}_i(\boldsymbol{r}) = \sum_{t=1}^N \alpha_t E_i(\boldsymbol{r}, \boldsymbol{r_t})$$

(2.a)

Under the assumed linear constitutive relationships, the *virtual* incident field $\mathcal{E}_i$ gives rise to a *virtual* contrast source $\mathcal{W}$

and a *virtual* scattered field $\mathcal{E}_s$ that are just a superposition of the original ones according to the same coefficients, i.e.:

$$\mathcal{W}(\boldsymbol{r}) = \sum_{t=1}^{N} \alpha_t \, W(\boldsymbol{r}, \boldsymbol{r}_t)$$

(2.b)

$$\mathcal{E}_s(\boldsymbol{r}_m) = \sum_{t=1}^{N} \alpha_t E_s(\boldsymbol{r}_m, \boldsymbol{r}_t)$$

(2.c)

Finally, by using Eqs. (2), Eqs. (1) can be recast for the VE as:

$$\mathcal{E}_s(\boldsymbol{r}_m) = \int_{\Omega} G_b(\boldsymbol{r}_m, \boldsymbol{r}') \, \mathcal{W}(\boldsymbol{r}') d\boldsymbol{r}' = \mathbb{A}_e[\mathcal{W}]$$

(3.a)

$$\mathcal{W}(\boldsymbol{r}) = \chi(\boldsymbol{r})\mathcal{E}_i(\boldsymbol{r}) + \chi(\boldsymbol{r}) \int_{\Omega} G_b(\boldsymbol{r}, \boldsymbol{r}') \, \mathcal{W}(\boldsymbol{r}') d\boldsymbol{r}'$$
$$= \chi\mathcal{E}_i + \chi\mathbb{A}_i[\mathcal{W}]$$

(3.b).

III. VIRTUAL EXPERIMENTS DESIGN

The design of a VE consists in determining the *virtual* excitation coefficients $\boldsymbol{\alpha}$. In doing so, the goal is that of enforcing some convenient properties of $\mathcal{W}$ that can be exploited in the inversion of Eqs. (3). As the actual contrast sources W are unknown and the scattered fields E_s collected in the original experiments are the only available data, the VE design must be based on these latter.

A first option is to formulate the design of a VE as the problem of synthesizing the coefficients $\boldsymbol{\alpha}$ such that the *virtual* incident field $\mathcal{E}_i$ interacting with the unknown targets produces a *desired virtual* scattered field pattern $\mathcal{E}_s^D$. To this end, let us introduce the multistatic response matrix (MSR) [17],[18], denoted with $\mathbb{K} \subset \mathbb{C}^{M \times N}$, which represents the $M \times N$ data matrix collected under the adopted measurements configurations. Its generic entry k_{ij} is the complex scattered field measured by the i-th receiver when the j-th transmitter is illuminating the region of interest. Moreover, let us express the recombination of the original data as follows:

$$\mathbb{K}\boldsymbol{\alpha} := \sum_{t=1}^{N} \alpha_t E_s(\boldsymbol{r}_m, \boldsymbol{r}_t)$$

(4)

and let us define $\boldsymbol{\mathcal{E}}_s^D \subset \mathbb{C}^M$ the vector containing the samples of the *desired virtual* scattered field $\mathcal{E}_s^D$ at the receivers locations. Then, the synthesis problem at hand can be expressed as:

$$\mathbb{K}\boldsymbol{\alpha} = \boldsymbol{\mathcal{E}}_s^D$$

(5)

As it is shown in Appendix A, this procedure can be related to the VE design approach based on LSM, exploited in [1]-[3]. In particular, Eq. (5) can be solved in the least square sense by computing the singular value decomposition (SVD) of $\mathbb{K}$. However, such inversion procedure is influenced by the presence of measurement noise which affects the elements of $\mathbb{K}$. As a countermeasure, only the singular values which are above of the noise level must be exploited to provide stable solution. However, since the noise level can be unknown, setting the proper truncation level of the SVD can be difficult. Moreover, the VE design based on (5) pursues the matching between the obtained *virtual* scattered field and the desired one, rather than directly reasoning on the *virtual* contrast source $\mathcal{W}$.

A. Direct design of virtual sources via adjoint operator

To overcome the above drawbacks, a different approach can be devised. Any radiated field is unambiguously paired with a purely radiating source, which is simply obtained via backpropagation [16]. This source is not exactly the one that radiates the field, but represents a convenient approximation of its radiating component[1]. Moreover, the computation of such a backpropagation source is straightforward, as it does not require any inversion process but a simple matrix multiplication.

In our case, the above circumstance entails that the *desired virtual* scattered field $\mathcal{E}_s^D$ is related to the *virtual* backpropagation contrast source $\mathcal{W}_{BP}^D$ as:

$$\mathcal{W}_{BP}^D(\boldsymbol{r}) = \sum_{m=1}^{M} [G_b(\boldsymbol{r}_m, \boldsymbol{r})]^* \mathcal{E}_s^D(\boldsymbol{r}_m) = \mathbb{A}_e^+[\mathcal{E}_s^D]$$

(6)

where * stands for the complex conjugate operation and $^+$ denotes the adjoint of the operator $\mathbb{A}_e$, such that $\langle \mathbb{A}_e[w], e \rangle = \langle w, \mathbb{A}_e^+[e] \rangle$, being $w \in L^2(\Omega)$ and $e \in L^2(\Gamma)$ [15].

From (6), it follows that we can recast the VE synthesis in terms of a desired, purely radiating, backpropagation contrast source $\mathcal{W}_{BP}^D$. From a formal point of view, this corresponds to apply the operator $\mathbb{A}_e^+$ to both sides of (5), as:

$$\mathbb{L}\boldsymbol{\alpha} = \mathbb{A}_e^+ \mathbb{K}\boldsymbol{\alpha} = \mathbb{A}_e^+ \left[\sum_{t=1}^{N} \alpha_t E_s(\boldsymbol{r}_m, \boldsymbol{r}_t) \right] =$$
$$= \sum_{t=1}^{N} \alpha_t \mathbb{A}_e^+ [E_s(\boldsymbol{r}_m, \boldsymbol{r}_t)] =$$
$$= \sum_{t=1}^{N} \alpha_t \, W_{BP}(\boldsymbol{r}, \boldsymbol{r}_t) = \mathcal{W}_{BP}{}^D(\boldsymbol{r})$$

(7)

where $\mathbb{L}$ is the compound operator $\mathbb{L} = \mathbb{A}_e^+ \mathbb{K} : L^2(\Gamma) \to L^2(\Omega)$

---

[1] Any source can be decomposed into a radiating part, a non-radiating part which corresponds to an identically null field outside of the source support and an essentially non-radiating part which gives rise to an evanescent field [16].

and $W_{BP}(\boldsymbol{r}, \boldsymbol{r_t}) = \mathbb{A}_e^+[E_s]$ is the backpropagation contrast source corresponding to the actual scattered field $E_s(\boldsymbol{r_m}, \boldsymbol{r_t})$ measured at $\boldsymbol{r_m}$ and due to the transmitter positioned in $\boldsymbol{r_t}$.

The last row of Eq. (7) provides a VE design equation directly cast in terms of *desired virtual* contrast sources. In particular, the superposition of the actual back-propagated contrast sources is forced to have the same behaviour in $\boldsymbol{r} \in \Omega$ as $\mathcal{W}_{BP}{}^D$.

As the operator $\mathbb{L}$ is compact, the synthesis problem cast in (7) is again ill-posed. While of course such a problem could be solved (with the same caveats) by adopting the same SVD-based regularization scheme used up to now to solve (5), a more straightforward procedure can be devised. Such procedure assumes as a solution of (7) the one provided by the application of the adjoint operator $\mathbb{L}^+$ to the right-hand member. Accordingly, a solution of (7) is readily obtained as:

$$\alpha_t = \mathbb{L}^+ \mathcal{W}_{BP}^D(\boldsymbol{r}) = \int_\Omega [W_{BP}(\boldsymbol{r}', \boldsymbol{r_t})]^* \mathcal{W}_{BP}^D(\boldsymbol{r}') d\boldsymbol{r}'$$

(8)

By observing that the right-hand member is a scalar product, Eq. (8) can be interpreted as follows: the amplitude of the α_t coefficients will be large for those actual experiments whose backpropagated currents are somehow similar (but for a scale factor) to the desired virtual one, while it will be relatively small or negligible for those backpropagated currents which are nearly orthogonal to the desired virtual one $\mathcal{W}_{BP}^D$.

The above approach is inspired by the adjoint synthesis method, introduced in [9],[10] as a convenient way to provide a purely radiating solution to the synthesis of an array. In our case, this method proves to be convenient for two reasons. The first one is that it provides an estimate of the solution without performing the inversion of the compact operator $\mathbb{L}$, which requires to use the error-affected SVD of $\mathbb{L}$. The second reason is that the adjoint solution provides an estimate of the sought unknown which, among all solutions with bounded norm, brings the better trade-off between accuracy and stability [9],[10].

It is worth noting that $\mathcal{W}_{BP}^D$ enforced in the designed VE is independent from the unknown targets (being in fact a degree of freedom of the design). On the other hand, $\mathcal{W}_{BP}^D$ is built as a linear combination via the coefficients α_t in (8), that are instead dependent on the target properties through W_{BP}. As such, in the designed VE, the "footprint" of the targets is encoded in the data-driven coefficients $\boldsymbol{\alpha}$.

In summary, the VE synthesis, exploited and tested in the following Sections, can be simply summarized as:

    1. Set the desired $\mathcal{W}_{BP}^D$.
    2. For $t = 1, .., N$
        Compute $W_{BP}(\boldsymbol{r}, \boldsymbol{r_t})$ for all transmitters, via $\mathbb{A}_e^+[E_s]$;
        Compute α_t for $\mathcal{W}_{BP}^D$ by using (8).
    3. Recombine E_i and E_s according to (2).

B. A closer look to the actually synthesized contrast sources

Eq. (8) is the key result of this paper, as it provides a direct formula to design a VE, in which the radiating component of the induced *virtual* contrast source has a prescribed behaviour within the investigated domain.

The radiating component of the contrast source plays an important role in the scattering phenomena, as it is responsible of the radiation. On the other hand, non-radiating sources are the cause of ill-posedness and non-uniqueness of the inverse source problem [16]. Accordingly, the reformulation of the inverse problem in the obtained VE framework (see Eqs. (3)) is expected to be more robust with respect to these two issues than the original problem (see Eqs. (1)).

This remarkable goal is not exactly accomplished, as the contrast source actually induced in the *virtual* experiment is given by (2.b), that is by the combination of the contrast sources W that have (or may have) a non-radiating component. However, as the *virtual* excitation coefficients $\boldsymbol{\alpha}$ are estimated via the adjoint operator, they are characterized by a bounded norm and are energetically optimal [9],[10]. As a consequence, they enforce *virtual* induced currents with bounded norm [19], whose non-radiating sources is not expected to play a dominant role.

A better understanding of the actually synthetized contrast sources can be achieved by replacing (8) in (2.b). By so doing, an explicit relationship for the actual *virtual* contrast sources is found, which reads:

$$\mathcal{W}(\boldsymbol{r}) = \int_\Omega \mathcal{W}_{BP}^D(\boldsymbol{r}') \sum_{t=1}^N W(\boldsymbol{r}, \boldsymbol{r_t})[W_{BP}(\boldsymbol{r}', \boldsymbol{r_t})]^* d\boldsymbol{r}'$$

(9)

Such relationship suggests that designed *virtual* contrast sources $\mathcal{W}$ is a weighted version $\mathcal{W}_{BP}^D$ according to the spatially varying factor given by the product on Γ between W and W_{BP}. Note that, if such product is equal to a delta function in $\boldsymbol{r}$, the *virtual* contrast sources $\mathcal{W}$ would be exactly equal to $\mathcal{W}_{BP}^D$.

By decomposing the actual currents $W(\boldsymbol{r}, \boldsymbol{r_t})$ in a backpropagated component W_{BP} and the residual (i.e., non-radiating and/or essentially non-radiating [16]) components $\Delta W(\boldsymbol{r}, \boldsymbol{r_t})$, the expression (9) can be recast as:

$$\mathcal{W}(\boldsymbol{r}) = \int_\Omega \mathcal{W}_{BP}^D(\boldsymbol{r}') g_1(\boldsymbol{r}, \boldsymbol{r}') d\boldsymbol{r}' + \int_\Omega \mathcal{W}_{BP}^D(\boldsymbol{r}') g_2(\boldsymbol{r}, \boldsymbol{r}') d\boldsymbol{r}'$$

(10)

wherein:

$$g_1(\boldsymbol{r}, \boldsymbol{r}') = \sum_{t=1}^N W_{BP}(\boldsymbol{r}, \boldsymbol{r_t})[W_{BP}(\boldsymbol{r}', \boldsymbol{r_t})]^*$$

(11.a)

$$g_2(\boldsymbol{r}, \boldsymbol{r}') = \sum_{t=1}^N \Delta W(\boldsymbol{r}, \boldsymbol{r_t})[W_{BP}(\boldsymbol{r}', \boldsymbol{r_t})]^*$$

(11.b)

Whatever r_t, each addendum of $g_1(r, r')$ is peaked in $r' = r$ [17],[18] and such a behavior is enhanced by the sum over the transmitter curve Γ. Conversely, each addendum of $g_2(r, r')$ may not exhibit such a property. Hence, the sum over Γ in (11.b) and the integration in Ω in (10) can cancel out or make negligible the contribution of ΔW to $\mathcal{W}$. As a consequence, as long as the effect of the second integral in (10) is negligible, one can assume that the actual virtual currents will be indeed an approximated version of the $\mathcal{W}_{BP}^D(r')$. Note that such a requirement is related to the contribution of the non-radiating and/or essentially non-radiating components of the actual currents, which are expected to increase with the amplitude of the contrast. As such, when higher and higher contrasts are considered, the adjoint procedure is expected to exhibit some limitations in the design of the desired currents.

All the above reasoning and arguments are fully supported by the ad hoc numerical tests reported in Section V, where we show that the proposed design procedure definitely outperforms the previous ones [1]-[3] .

IV. CIRCULARLY SYMMETRIC VIRTUAL SOURCES

To give an example of the VE design procedure described in the previous Section, let us consider the case of VE enforcing *virtual* contrast sources having a circular symmetry with respect to a set of properly selected *pivot points* r_p, and corresponding to elementary currents herein located. Note that this is the case so far considered in the VE design using LSM [20] (see also Appendix A).

To this end, let us recall that, in the case we are considering of a homogenous medium, the backpropagated contrast source $\mathcal{W}_{BP}^D$ can be expressed in a closed form [16] as:

$$\mathcal{W}_{BP}^D(r, r_p) = \mathbb{A}_e^+[G_b(r_m, r_p)] = \beta J_0(k_b|r - r_p|)$$
(12)

wherein G_b exactly corresponds to the field radiated on $r_m \in \Gamma$ by an elementary source positioned in the pivot point r_p, J_0 is the Bessel function of zero order and β is a constant, which does not depend on r and r_p, and modulates the amplitude of J_0.

Accordingly, one has just to replace (12) in (8) to obtain the desired coefficients, after the W_{BP} have been computed via $\mathbb{A}_e^+$.

To complete the design procedure, the choice of the pivot points r_p, which are needed to provide a set of VE, must be discussed. In this respect, as the contrast source is defined only for $\chi \neq 0$, it is obvious that the pivot points must be picked within the support of the targets, as otherwise $\mathcal{W}^D$ would be null in the pivot point.

The selection of the pivot points according to the above basic principle is straightforward in the case of circularly symmetric virtual contrast sources. As a matter of fact, as shown in Appendix B, the expression of α given by (8) is related to the orthogonality sampling method [11]-[13], a well-known qualitative imaging method. In particular, the energy (l_2-norm) of α corresponds to the indicator function used in the OSM to estimate the targets support, which attains large values when r_p

belongs to the support of the targets and low values elsewhere [11]. As such, by plotting the l_2-norm of α, that is $\|\alpha\|_\Gamma^2$, on the entire imaging domain Ω, it is possible to determine the unknown target's support and use this information to select the pivot points to be used in the design of the VE.

In conclusion, by means of the proposed approach, the synthesis of circularly symmetric sources is performed as:

1. *Set the desired* $\mathcal{W}_{BP}^D = \mathbb{A}_e^+[G_b(r_m, r_p)]$.
2. *Determine* $W_{BP}(r, r_t)$ *via* $\mathbb{A}_e^+[E_s]$;
3. *Compute* $\|\alpha\|_\Gamma^2$ *using (8) for an arbitrary set of points* r_s *sampling* Ω *to estimate the target support.*
4. *Select the pivot points* r_p *within the estimated support and pick the corresponding coefficients* α *to build the desired VE.*
5. *Recombine* E_i *and* E_s *according to (2).*

V. ASSESSING THE NEW VE DESIGN PROCEDURE

In this Section, numerical tests of the capability of Eq. (8) to design VE enforcing circularly symmetric *virtual* contrast sources are reported. In particular, a comparison with the so far exploited LSM-based design is pursued.

The first test scenario consists of a lossless cylindrical object of radius of ~$0.33\lambda_b$ with $\chi = 1$, embedded in a homogenous medium within a square domain of side $L = 1.5\,\lambda_b$ discretized into 64×64 cells [21], being λ_b the wavelength in the background. Moreover, without loss of generality, we assume $r_m = r_t$. According to the Nyquist criterion suggested in [16], $N = M = 15$ incident directions and measurements (collected on a circumference Γ of radius $R = 3\lambda_b$) have been considered. The scattered field data, simulated by means of a full-wave solver based on the method of moments, have been corrupted with a random Gaussian noise with SNR = 20 dB.

In Figures 2(a) and 2(b), the normalized values of $\|\alpha\|_\Gamma^2$ computed via LSM and (8) are reported, respectively. In these figures, r_s spans all the points belonging to the grid which samples the investigation domain Ω. Figures 2(c)-(f) and 2(g)-(j) show the amplitudes of the *virtual* contrast sources $\mathcal{W}$ designed by means of LSM and adjoint solution (8), respectively, for some pivot points r_p. As can be seen, when the pivot point belongs to the support, focused and circularly symmetric contrast sources are induced. Conversely, when the pivot point does not belong to the support, the contrast source does not show any circular symmetry (see Fig.s 2(f),(j)). This circumstance holds true whatever the design approach.

By comparing the plots in Figure 2, it turns out that the adjoint solution (8) not only allows a simpler VE design, but also is able to enforce a better circular symmetry. Indeed, it avoids the deformation of the circular pattern of the currents, especially when the pivot point is close to the boundary of the target (see Figs. 2(d),(e) and 2(h),(i)). Indeed, the circular pattern obtained via Eq. (8) preserves the regularity of the desired currents $\mathcal{W}_{BP}^D$ (see Figs. 2(k)-(n)), even if it shrinks, possibly due to unavoidable presence of a small amount of non-radiating currents.
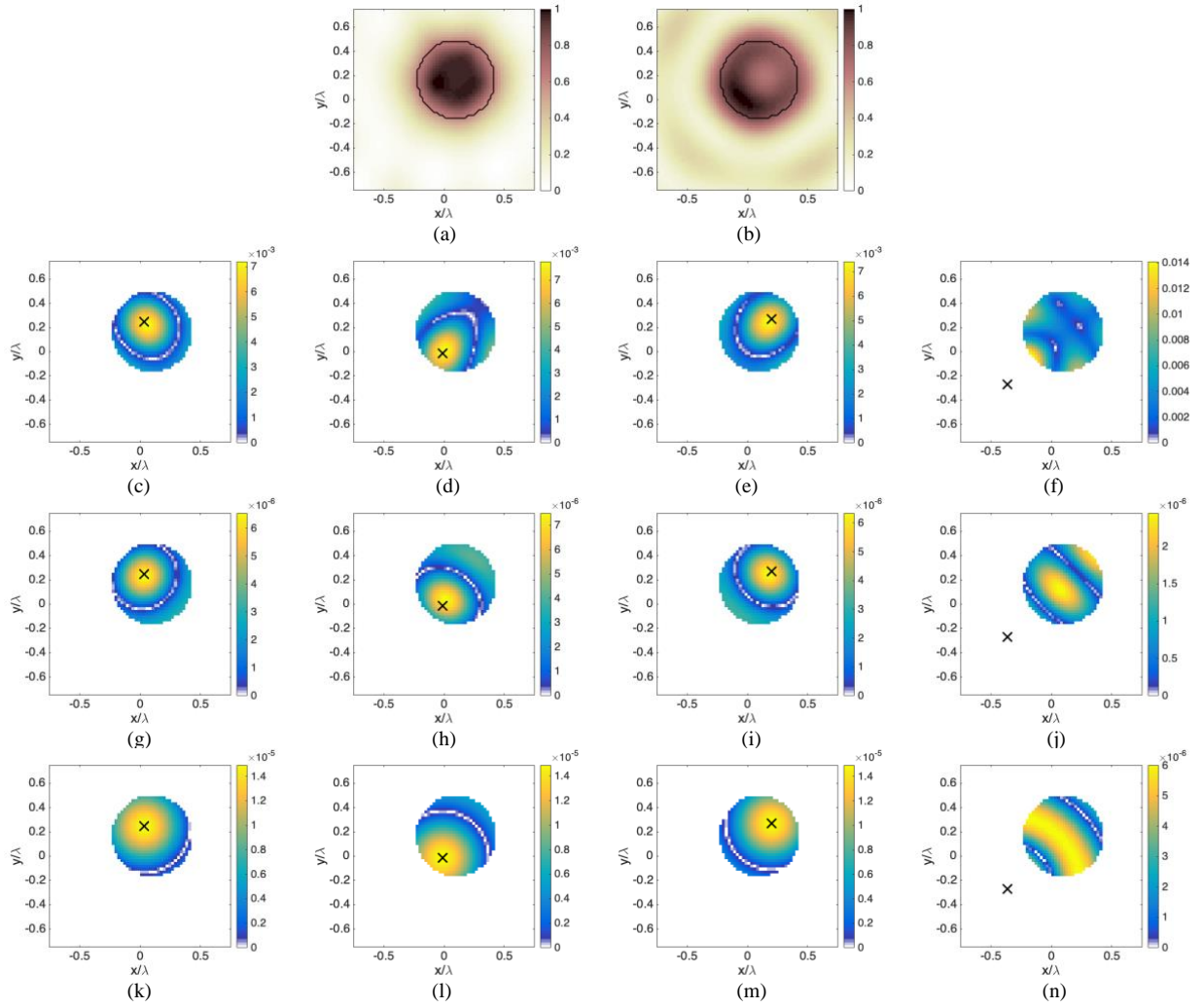
Figure 2. Numerical validation of the proposed VE design strategy: the cylindrical target. SNR= 20 dB. Retrieved supports via LSM (a) and adjoint solution (b). Amplitudes of virtual induced currents $\mathcal{W}$ for some pivot points via LSM (c)-(f) and adjoint solution (g)-(j). Amplitudes of desired currents $\mathcal{W}_{BP}^{D}$ (k)-(n).The pivot points are superimposed as black crosses: (c),(g),(k) r_p=(0.035 λ_b,0.24 λ_b), (d),(h),(l) r_p=(-0.012 λ_b, -0.012 λ_b), (e),(i),(m) r_p=(0.20 λ_b, 0.27λ_b), (f),(j),(n) r_p=(-0.36 λ_b, -0.27 λ_b).

$r_p = (x_p, y_p)$	LSM based VE design		adjoint VE design	
	SNR=20 dB	SNR=10 dB	SNR=20 dB	SNR=10 dB
(0.035 λ_b,0.24 λ_b)	14	20	3	6
(-0.012 λ_b, -0.012 λ_b)	63	58	42	46
(0.20 λ_b, 0.27λ_b)	29	30	10	13

Table I. The synthetic parameter sym pertaining to the virtual currents induced in the cylindrical target.

To quantitatively appraise the difference in terms of circular pattern of the currents, a synthetic parameter, defined as the l_2-norm of the angular derivative ∂_ϑ of the *virtual* contrast sources, has been computed as:

$$sym(r_p) = \left\| \partial_\vartheta [\mathcal{W}(r, r_p) \Pi(r, r_p)] \right\|_2^2 \tag{13}$$

wherein ϑ is the angular coordinate of a local polar reference system centered in r_p and $\Pi(r, r_p)$ identifies a circular neighborhood of radius 0.3 λ_b. The larger the value of sym, the worse the circular symmetry around the considered pivot point. As can be seen from the values are reported in Table I, the new design approach improves the symmetry parameter sym of roughly the 50% on average, thus confirming the reasoning in Section III.

As a second test case, a lossy 'kite' target with $\chi = 1.2 - 0.36\,i$ and leading dimension of λ_b, embedded in a homogenous medium, has been considered. The square domain of side $L =$
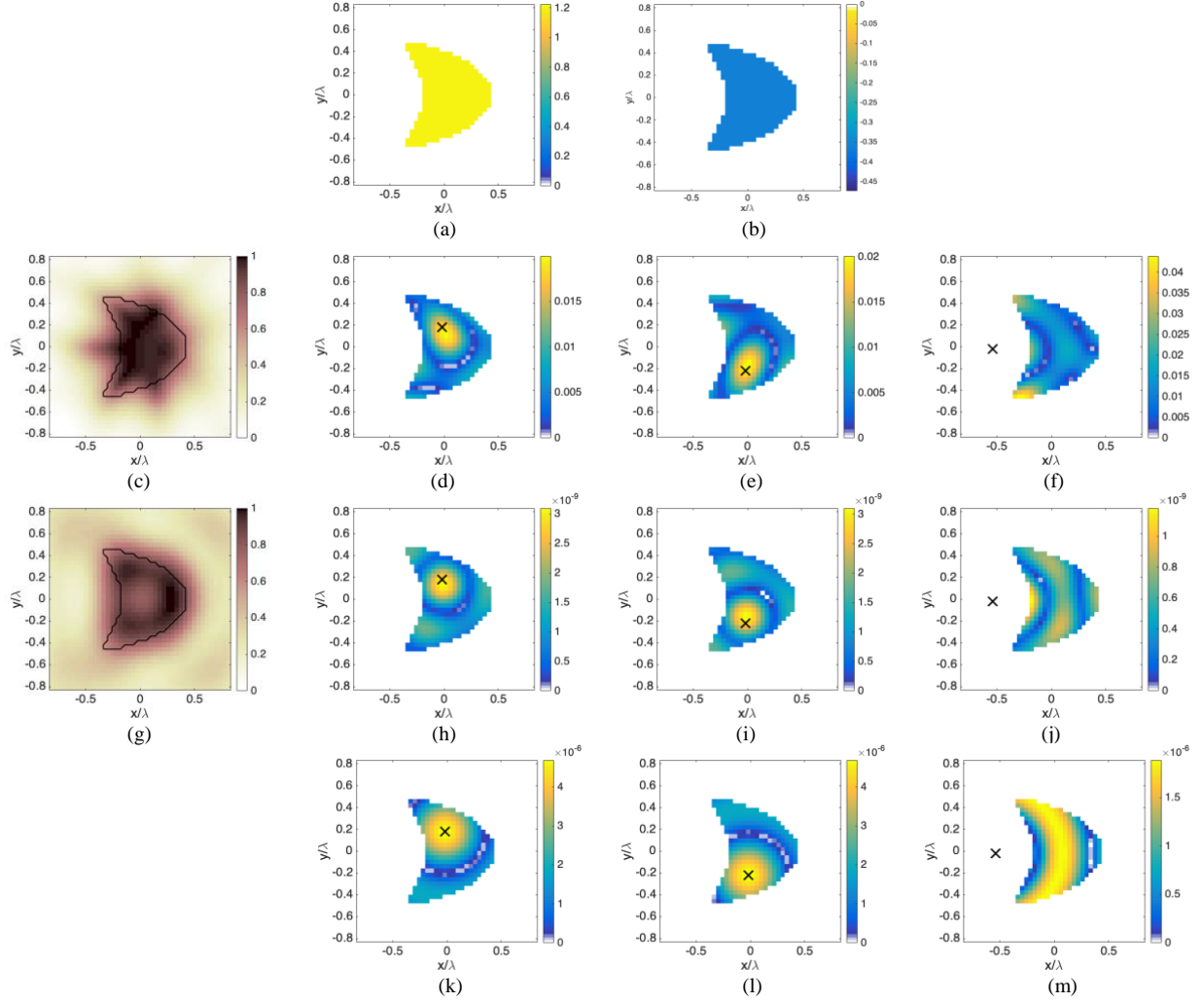
Figure 3. Numerical validation of the proposed VE design strategy: the kite target. SNR= 20 dB. Real part and imaginary part of the contrast function (b)-(c). Retrieved supports via LSM (c) and adjoint solution (g). Amplitudes of virtual induced currents $\mathcal{W}$ for some pivot points via LSM (d)-(f) and adjoint solution (h)-(j). Amplitudes of desired currents $\mathcal{W}^D_{BP}$ (k)-(m).The pivot points are superimposed as black crosses: (d),(h),(k) r_p=(-0.02 λ_b,0.18 λ_b), (e),(i) , (l) r_p=(-0.02 λ_b, -0.22 λ_b), (f),(j),(m) r_p=(-0.53 λ_b, -0.02 λ_b).

$r_p = (x_p, y_p)$	LSM based VE design			adjoint VE design		
	SNR=20 dB	SNR=10 dB	SNR=5 dB	SNR=20 dB	SNR=10 dB	SNR=5 dB
(-0.02 λ_b,0.18 λ_b)	32	33	36	10	10	13
(-0.02 λ_b, -0.22 λ_b)	33	34	37	20	20	22

Table II. The synthetic parameter *sym* pertaining to the virtual currents induced in the kite target.

1.66 λ_b has been discretized in 42×42 cells [21] (see Figs. 2(a)-(b)). Moreover, $N = M = 22$ (according to the Nyquist rule), $R = 4 \lambda_b$ and SNR = 20 dB. In Figures 3(c) and 3(g) the normalized values of $\|\alpha\|^2_F$ computed with LSM and adjoint solutions are respectively reported, while Figures 3(d)-(f) and 3(h)-(j) show the amplitudes of the designed *virtual* contrast sources.

By comparing Figs. 3(e) and 3(i) it turns out that the VE design exploiting the adjoint solution again avoids the deformation of the circular pattern of the currents (see Table II).

Indeed, one can notice that the adjoint solution (8) allows to preserve the same regularity of the pattern of $\mathcal{W}^D_{BP}$ (see Fig.s 3(k)-(m)), while also outperforming the LSM in support retrieval. Again, this improved performance confirms the discussion in Section III.

In order to show the increased robustness to noise of the proposed design method with respect to the one based on the LSM, the examples in Figures 2 and 3 have been re-run with different SNR. The results in term of synthetic parameter *sym* are summarized in the Tables I and II.
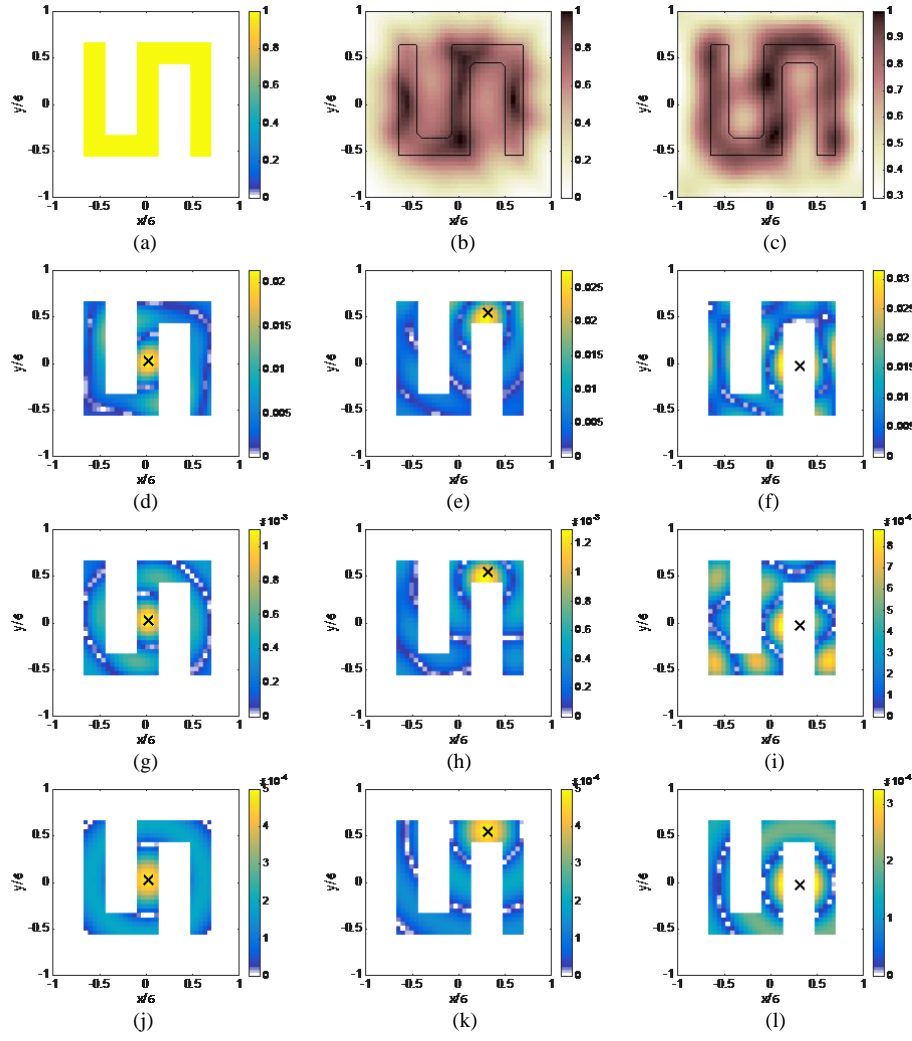
Figure 4. Numerical validation of the proposed VE design strategy: the lossless S shaped target. Real part of the contrast function (a). Retrieved supports via LSM (b) and adjoint solution (c). Amplitudes of virtual induced currents $\mathcal{W}$ for some pivot points via LSM (d)-(f) and adjoint solution (g)-(i). Amplitudes of desired currents $\mathcal{W}_{BP}^{D}$ (j)-(l).The pivot points are superimposed as black crosses: (d),(g),(j) r_p=(-0.024 λ_b,0.024 λ_b), (e),(h),(k) r_p=(0.31 λ_b, 0.60 λ_b), (f),(i),(l) r_p=(0.31 λ_b, -0.024 λ_b).

$r_p = (x_p, y_p)$	LSM based VE design	adjoint VE design
(-0.024 λ_b,0.024 λ_b)	13	11
(0.31 λ_b, 0.60 λ_b)	22	20

Table III. The synthetic parameter sym pertaining to the virtual currents induced in the S shaped target.

Finally, stimulated by a reviewer's comment, the lossless S shaped target embedded in free space has been considered (see Figs. 4(a)). The square domain of side $L = 2\,\lambda_b$ has been discretized in 42×42 cells [21]. Moreover, $N = M = 19$, $R = 2\,\lambda_b$ and SNR = 20 dB. The results are shown in Figure 4 and Table III. As can be seen, notwithstanding the complex shape of the target, both LSM and adjoint solutions can synthesize the desired currents. Notably, the adjoint solution provides an improved circular symmetry of the currents and better estimates the target support, which also leads (see the next section) to a better quantitative inversion.

VI. NUMERICAL TESTS: INVERSION BASED ON NEW VE DESIGN

In this Section, some results of quantitative profiling achieved using the VE designed via solution (8) are reported. In particular, among the different VE-based inversion procedures which have been introduced in literature, we focus our attention on the *direct algebraic reconstruction* (DARE) proposed in [2]. The DARE approach takes advantage of two main ideas. First, the original scattering experiments are re-arranged to give rise to *virtual* contrast sources focused in a set of pivot points
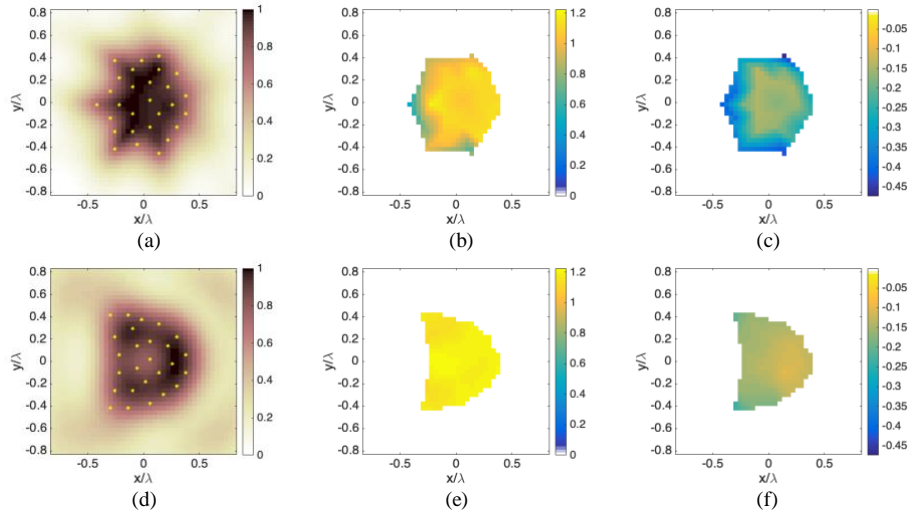
Figure 5. Inversion through the proposed VE design strategy: the kite target. Retrieved supports via LSM (a) and adjoint solution (d) with the selected pivot points superimposed as dots. Real part and imaginary part of the contrast functions retrieved via LSM-DARE (b)-(c) and via Ad-DARE (e)-(f).
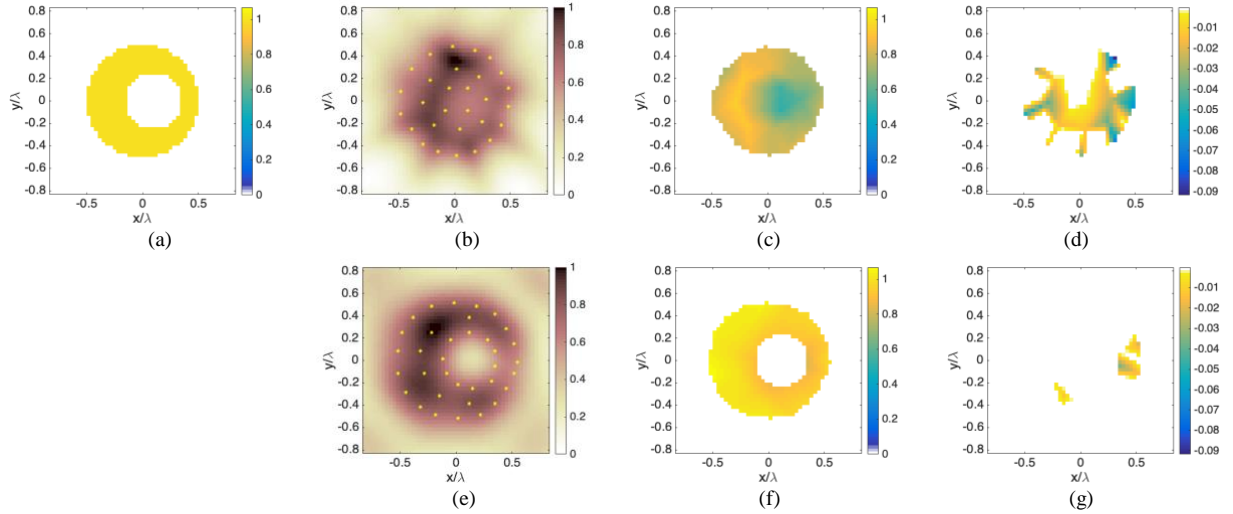

Figure 6. Inversion through the proposed VE design strategy: the non-convex target. Real part of the reference contrast profile (a). Retrieved support via LSM (b) and adjoint solution (e) with the selected pivot points superimposed as dots. Real part and imaginary part of the contrast functions retrieved via LSM-DARE (c)-(d) and via Ad-DARE (f)-(g).

belonging to the imaged domain. Then, an analytical approximation is introduced for the *virtual* contrast sources, which holds true in a neighbourhood of the pivot point. Such an approximation relies on a theorem for Bessel functions and provides an explicit dependence of the focused *virtual* contrast sources on the contrast function. Note this approximation can be used when the contrast function is assumed to be slowly variable around each pivot point [2].

These two simple ideas allow recasting the inverse problem in such a way that the values of the contrast in the pivot points can be achieved by solving a diagonal system of algebraic equations of the kind:

$$A(X \odot X \odot X) + B(X \odot X) + CX + D = 0$$

(14)

where $\odot$ denotes the Hadamard product between vectors, $X = [\chi_1 \cdots \chi_k \cdots \chi_P]^T$ is the vector that contains the punctual

values of the unknown contrast in the selected pivot points r_p, and $(\cdot)^T$ denotes the matrix transposition. Finally, A, B, C and D are diagonal matrices whose expressions are known and can be found in [2]. The solution of (14) provides the values of the contrast function in the considered pivot points. Then, these latter are interpolated in order to achieve the overall image of the target. As a consequence, provided the proposed approximation holds true, the inverse scattering problem is solved by means of closed form formulas, and, hence, in a deterministic and computationally very effective way.

In [2] DARE has been tested using LSM-designed VE, whereas in the following we assess its capabilities and performance using VE designed via Eq. (8). In what follows, we refer to the first approach as LSM-DARE, while the one proposed here is referred as Adjoint-DARE (Ad-DARE).

A. Simulated data

As first example, we have again considered the lossy kite shown in Figure 3. Figs. 5(a) and 5(d) show the retrieved support with the considered pivot points superimposed for LSM-DARE and Ad-DARE, respectively. In both cases the VE have been designed with respect to the selected pivots using the relevant formula. Finally, the diagonal system of third-degree algebraic equations described in Eq. (14) has been solved.

The retrieved contrast functions, resulting from the linear interpolation of the punctual values estimated in the selected pivot points, obtained via LSM-DARE and Ad-DARE are shown in Figs. 5(b),(c) and 5(e),(f), respectively. As can be seen, due to the better estimation of the target support, Ad-DARE outperforms LSM-DARE in retrieving the target. To quantitatively appraise such a qualitative observation, we computed the normalized mean square error between the retrieved contrast function $\tilde{\chi}$ and the actual one χ, that is:

$$NMSE = \frac{\|\chi - \tilde{\chi}\|_2^2}{\|\chi\|_2^2}$$

(14)

The NMSE is 0.28 for LSM-DARE, while it is as low as 0.18 in case of Ad-DARE.

As second example, a non-convex lossless target with $\chi = 1$ and dimension of λ_b has been considered (see Figure 6). The square domain of side $L = 1.66 \lambda_b$ has been discretized in 50×50 cells. Moreover, N=M=16, $R = 3.3\lambda_b$ and SNR = 15 dB. The retrieved support with the considered pivot points superimposed are shown in Figs. 6(b) and 6(e) for LSM-DARE and Ad-DARE, respectively, while the retrieved contrast functions are shown in figs 6(c),(d) and 6(f),(g). Note that in this example the punctual values X obtained via Ad-DARE are interpolated by taking into account the corresponding support estimation. As can be seen, a better accuracy in the contrast reconstruction is reached, as also witnessed by the NMSE (0.16 against 0.29).

Finally, as last example with simulated data, the lossless target in Figure 4 has been considered. The results are reported in Figure 7 and show that, even if the LSM-DARE reaches a slightly lower error, the reconstruction via Ad-DARE allows a better rendering in terms of shape and homogeneity of the electrical properties.

Note that in the above cases the overall inversion procedure involved in Ad-DARE takes just one or two seconds. The numerical calculations have been run on a workstation equipped with one Intel i5 (2.9 GHz) processor and 8 GB RAM.

B. Experimental data

In this subsection we assess the Ad-DARE against the Fresnel experimental data [22], which are usually adopted to benchmark inverse scattering procedures. As compared with previous examples using simulated data, the Fresnel experiments introduce the additional difficulty of dealing with a partially aspect limited configuration. More details about the measurement configuration and the target are reported in [22]. Among the different targets belonging to the Fresnel dataset, the *TwinDiel* target has been considered [22]. It consists of two identical purely dielectric circular cylinders with radius 1.5 cm and contrast $\chi = 2 \pm 0.3$. The herein processed data are

organized in a 72×36 matrix by simply replacing with zeros the original data entries that are not available. The investigated domain is a square of side 0.15 m and the working frequency is 6 GHz.

The retrieved support with the considered pivot points superimposed are shown in Figs. 8(a) and 8(d) for LSM-DARE and Ad-DARE, respectively. The retrieved contrast functions are shown in Figs. 8(b)-(c) and 8(e)-(f). Note that the punctual values X are interpolated by taking into account the corresponding supports. Although no quantitative metric can be given in this case, the results clearly allow to appreciate how Ad-DARE allows to improve the already good result achieved with LSM-DARE, thus confirming the effectiveness of the underlying VE design procedure.

VII. CONCLUSION

In this contribution, the problem of designing *virtual* scattering experiments (VE) has been addressed and pursued by means of a simple yet effective design approach.

The proposed design procedure is innovative with respect to the one so far exploited, as it allows to directly design the *virtual* currents in such a way to exhibit desired features. Moreover, it is general as it can be used for a generic desired currents distribution. In particular, as long as the effect of the non-radiating currents is cancelled out, one can assume that the actual virtual currents is an approximated version of the desired one.

The presented tests have shown the reliability and effectiveness of the approach in the specific case of focused *virtual* currents and homogeneous medium. However, the proposed design approach can be applied to more complex scenarios as well as to different kind of *nominal* currents, such as for instance the one radiating the higher order multipoles, as suggested in [8],[23],[24]. Furthermore, the proposed design procedure is straightforward as it does not require an explicit regularization and inversion process, but just the evaluation of the adjoint solution of the VE design equation. As such, it is much more stable with respect to the noise and also energetically optimal [9],[10].

As far as the computational burden, in the *adjoint* VE design procedure, the calculation of the SVD of the measured data is avoided. As such, the *adjoint* VE design, combined with the very fast DARE method, allows to get a very fast overall inversion procedure.

Finally, the recognized connection between the proposed procedure and the OSM has a number of interesting consequences. First, OSM is more reliable in retrieving the target support, so that selection of pivot points can be more accurate. Second, as shown in [25], OSM is capable to provide qualitative information on the behavior of the permittivity (e.g. step-like) so that such an information can be encoded in the inversion as well as in the pivot selection.

Future work will aim at exploiting the proposed procedure in case of different desired currents as well as analysing the limitations with respect to the case of large contrast profile. Moreover, numerical tests in complex scenario and in conjunction with other imaging techniques will be performed.
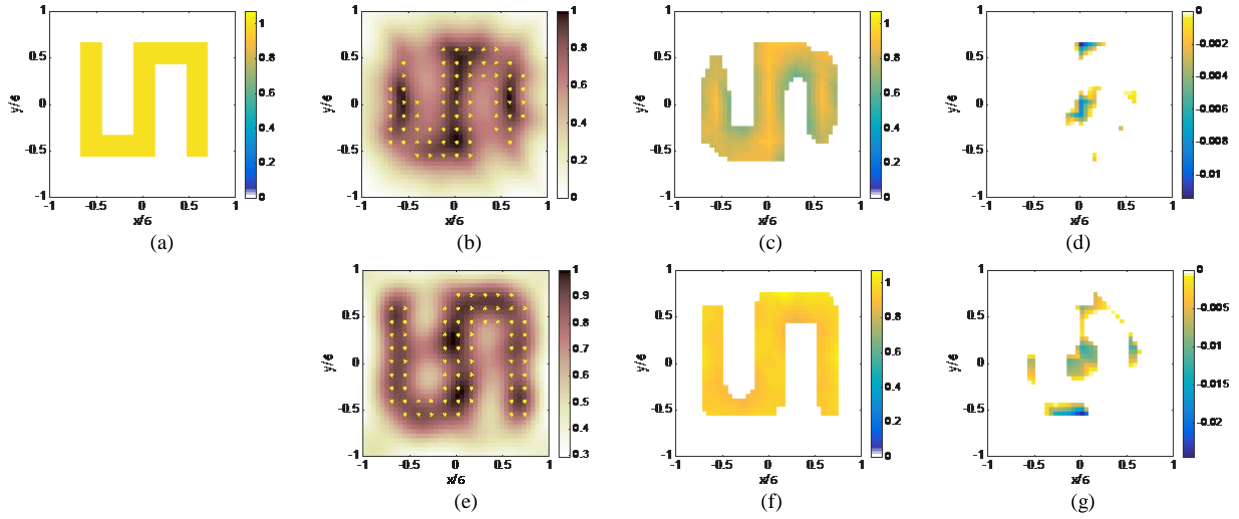
Figure 7. Inversion through the proposed VE design strategy: the lossless S shaped target. Real part of the reference contrast profile (a). Retrieved support via LSM (b) and adjoint solution (e) with the selected pivot points superimposed as dots. Real part and imaginary part of the contrast functions retrieved via LSM-DARE (NMSE= 0.32) (c)-(d) and via Ad-DARE (NMSE=0.36) (f)-(g).
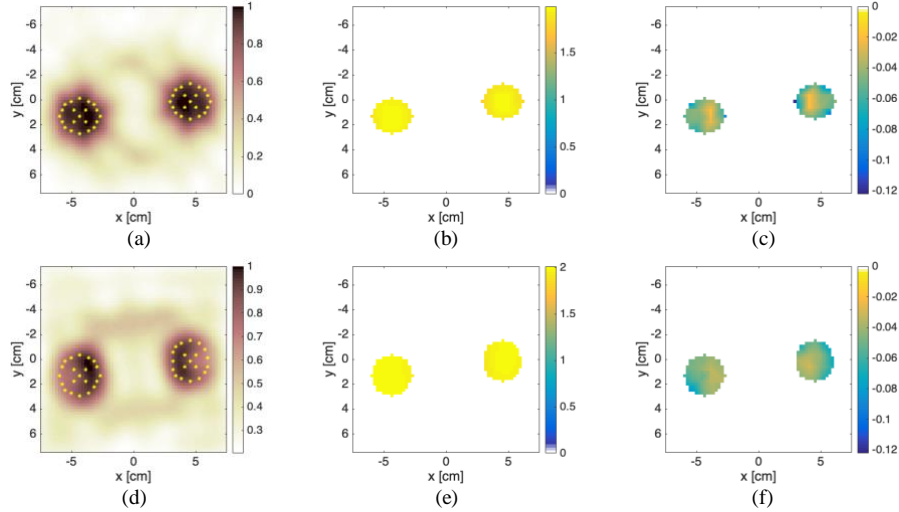

Figure 8. Inversion through the proposed VE design strategy: the *TwinDiel* Fresnel target. Retrieved support via LSM (a) and adjoint solution (b) with the selected pivot points superimposed as yellow dots. Real part and imaginary parts of the contrast functions retrieved via LSM-DARE (b)-(c) and via Ad-DARE (e)-(f).

APPENDIX A

In case of circularly symmetric VE design, the vector $\mathcal{E}_s^D \subset \mathbb{C}^M$ contains the sample of the field radiated by an elementary source located in r_p, that is $G_b(r_m, r_p)$. Then, equation (5) exactly corresponds to the (discretized) far field integral equation underlying the LSM [20], whose direct solution is not possible owing to ill-conditioning and a regularization technique is required.

A possible solution of problem (5) can be achieved by minimizing in a least square sense the residual between $\mathbb{K}\alpha$ and $\mathcal{E}_s^D$, that is:

$$\min\phi = \min_{\alpha}\|\mathbb{K}\alpha - \mathcal{E}_s^D\|_\Gamma^2$$

(A.1)

and using the Tikhonov regularization [15]. This solution exactly corresponds to the one so far exploited in the VE design [1]-[3], that is:

$$\alpha_t(r_p) = \sum_k \frac{\lambda_k}{\lambda_k^2 + \gamma^2}\langle G_b(\hat{r}_m, r_p), u_k(\hat{r}_m)\rangle_\Gamma v_k(\hat{r}_t)$$

(A.2)

wherein $\{u_k, \lambda_k, v_k\}$ is the SVD of the operator $\mathbb{K}$ and γ is the Tikhonov regularization parameter, whose selection is crucial in order to obtain stable and reliable *virtual* excitation coefficients [15].

APPENDIX B

Let us substitute Eq. (12) in (8) to express the generic coefficient α_t as:

$$\alpha_t(\boldsymbol{r_p}) = \beta \int_\Omega J_0\big(k_b|\boldsymbol{r} - \boldsymbol{r_p}|\big)[W_{BP}(\boldsymbol{r}, \boldsymbol{r_t})]^* d\boldsymbol{r}$$

(B.1)

Due to the properties of the Bessel function, which is able to filter out the spectral components only located in a circle of radius k_b [25], equation (B.1) can be rewritten in term of original induced currents, that is:

$$\alpha_t(\boldsymbol{r_p}) = \beta \int_\Omega J_0\big(k_b|\boldsymbol{r} - \boldsymbol{r_p}|\big)[W(\boldsymbol{r}, \boldsymbol{r_t})]^* d\boldsymbol{r}$$
$$= \beta \left[\int_\Omega J_0\big(k_b|\boldsymbol{r} - \boldsymbol{r_p}|\big)W(\boldsymbol{r}, \boldsymbol{r_t})\right]^* d\boldsymbol{r}$$

(B.2)

The last term of (B.2) corresponds to the complex conjugate of the so-called *reduced scattered field* E_s^{red}. In OSM, such a field tests the *orthogonality* relation between the far-field pattern and the Green's function in the far zone, [11],[25].

The OSM images the target shape via the computation of the energy associated to the *reduced scattered field* [11], that is $\left\|E_s^{red}(\boldsymbol{r_p}, \boldsymbol{r_t})\right\|_\Gamma^2$. Such energy achieves large values when the far-field pattern approaches the one of the background Green's function for the considered sampling point, that is when the point $\boldsymbol{r_p}$ belongs to the target support [11].

Since $\|\alpha_t\|_\Gamma^2 \propto \left\|E_s^{red}(\boldsymbol{r_p}, \boldsymbol{r_t})\right\|_\Gamma^2$, we can conclude that the energy of the *virtual* excitation coefficient α_t allows to identify the target support.

REFERENCES

[1] L. Crocco, I. Catapano, L. Di Donato and T. Isernia, "The Linear Sampling Method as a Way to Quantitative Inverse Scattering," in *IEEE Transactions on Antennas and Propagation*, vol. 60, no. 4, pp. 1844-1853, April 2012.

[2] M. T. Bevacqua, L. Crocco, L. Di Donato, T. Isernia, An Algebraic Solution Method for Nonlinear Inverse Scattering, *IEEE Trans on Ant Prop*, 63(2): 601,610, 2015.

[3] L. Di Donato, M. T. Bevacqua, L. Crocco and T. Isernia, "Inverse Scattering Via Virtual Experiments and Contrast Source Regularization," *IEEE Trans. Antennas Propag.*, vol. 63, no. 4, pp. 1669-1677, April 2015.

[4] D. Colton and R. Kress. Inverse Acoustic and Electromagnetic Scattering Theory, *Springer-Verlag*, Berlin, Germany, 1998.

[5] Cakoni, F. and D. Colton, *Qualitative Methods in Inverse Scattering Theory*, Springer-Verlag, Berlin Heidelberg, 2006

[6] Kirsch, A.; Grinberg, N.I. *The Factorization Method for Inverse Problems*; Oxford University Press: Oxford, UK, 2008

[7] S. C. Pavone, G. Sorbello, L. Di Donato, On the Orbital Angular Momentum Incident Fields in Linearized Microwave Imaging, *Sensors*, vol. 20, n.7, 2020.

[8] L. Di Donato, M. T. Bevacqua, A. F. Morabito and T. Isernia, "Orbital Angular Momentum and Virtual Experiments for Microwave Imaging," *2019 PhotonIcs & Electromagnetics Research Symposium - Spring (PIERS-Spring)*, Rome, Italy, 2019, pp. 560-565.

[9] Dymski, V.N., Choni, Y.I. An approximate solution of problems of antenna synthesis allowing experimental simulation. *Radiophys Quantum Electron*, vol. 13, pp. 1069–1075, 1970.

[10] Y. I. Choni, "Adjoint operator method and its aspects in regard to antenna synthesis," IX International Conference on Antenna Theory and Techniques, Odessa, 2013, pp. 86-91, 2013.

[11] R. Potthast, "A study on orthogonality sampling", *Inverse Prob.*, 26(7): 2010.

[12] R.Griesmaier, "Multi-frequency orthogonality sampling for inverse obstacle scattering problems", *Inverse Probl.*, vol. 27, 2011.

[13] M. T. Bevacqua, R. Palmeri, T. Isernia and L. Crocco, "Exploiting the orthogonality sampling method to design virtual scattering experiments," *12th European Conference on Antennas and Propagation (EuCAP 2018)*, London, 2018, pp. 1-4.

[14] M. Pastorino, " Microwave Imaging", *John Wiley*, New York, May 2010.

[15] M. Bertero and P. Boccacci, "Introduction to Inverse Problems in Imaging", *Institute of Physics*, Bristol, UK, 1998.

[16] A. J. Devaney, Mathematical Foundations of Imaging, Tomography and Wavefield Inversion, Cambridge, 2012.

[17] F.K.. Gruber, E.A. Marengo and A.J. Devaney, "Time-reversal imaging with multiple signal classification considering multiple scattering between the targets", J. Acoust. Soc. Am., Vol. 115, pp. 3042-3047, 2004.

[18] M. Fink, "Time reversal of ultrasonic fields. i. basic principles," *IEEE Trans. Ultrason. Ferroelectr. Freq. Control.*, vol. 39, pp. 555–566, 1992.

[19] L. Crocco, L. Di Donato, D. A. M. Iero and T. Isernia, "A New Strategy to Constrained Focusing in Unknown Scenarios," in *IEEE Antennas and Wireless Propagation Letters*, vol. 11, pp. 1450-1453, 2012.

[20] D. Colton, H. Haddar, and M. Piana, "The linear sampling method in inverse electromagnetic scattering theory," Inverse Problems, vol. 19, pp. 105–137, 2003.

[21] J. Richmond, "Scattering by a dielectric cylinder of arbitrary cross section shape," *IEEE Trans. Antennas Propag.*, vol. 13, no. 3, pp. 334-341, 1965.

[22] K. Belkebir, M. Saillard, Special section: Testing inversion algorithms against experimental data. *Inverse Probl.*, *17*, 1565–2028, 2001.

[23] K. Agarwal, X. Chen, and Y. Zhong, "A multipole-expansion based linear sampling method for solving inverse scattering problems," *Opt. Express*, vol. 18, pp. 6366-6381, 2010.

[24] L. Crocco, L. Di Donato, I. Catapano, and T. Isernia, "An improved simple method for imaging the shape of complex targets," *IEEE Trans. Antennas Propag.*, vol. 61, no. 2, pp. 843–851, Feb. 2013.

[25] M. T. Bevacqua, T. Isernia, R. Palmeri, M. N. Akinci and L. Crocco, "Physical Insight Unveils New Imaging Capabilities of Orthogonality Sampling Method," in *IEEE Trans. Antennas Propag.*, vol. 68, no. 5, pp. 4014-4021, May 2020.